Comparison of Impedance Spectroscopy Expressions and Responses of Alternate Anomalous Poisson−Nernst−Planck Diffusion Equations for Finite-Length Situations

J. Ross Macdonald,[*,†] Luiz Roberto Evangelista,[‡] Ervin Kaminski Lenzi,[‡,§] and Giovanni Barbero[§]

[†]Department of Physics and Astronomy, University of North Carolina, Chapel Hill, North Carolina 27599, United States
[‡]Departamento de Física, Universidade Estadual de Maringá, Avenida Colombo, 8790, 87020-900 Maringá, Paraná, Brazil
[§]Dipartimento di Fisica, Politecnico di Torino, Corso Duca degli Abruzzi 24, 10129 Torino, Italy

ABSTRACT: Two empirical, but plausible, previously published independent general-izations of the standard Poisson−Nernst−Planck (PNP) continuum diffusion model for mobile-charge conduction in liquids and solids are discussed, their responses are compared, and their physical appropriateness and usefulness for data fitting are investigated. They both involve anomalous diffusion of PNPA type with power-law frequency-response elements involving fractional exponents. Both models apply to finite-length regions of material between completely blocking electrodes and, for simplicity, deal primarily with positive and negative charge carriers of equal valence numbers and mobilities. The charge carriers may be either ionic or electronic. The first PNPA model, model A, involves the common separation of the expression for ordinary PNP impedance into an interface diffusion part and a high-frequency limiting conductance and capacitance, followed by the replacement of all normal diffusion elements in the former by anomalous ones. It predicts the presence of the usual PNP plateau in the real part of the total impedance below the Debye relaxation frequency, followed at sufficiently low frequencies by an anomalous-diffusion power-law increase above the plateau. The second model, C, alternatively generalizes the normal time derivatives in the continuity equation by replacing them with fractional ones and leads to no plateau, except in the PNP limit, but instead predicts an immediate power-law increase as the frequency decreases below the Debye relaxation one. Fitting of experimental frequency response data sets for three disparate materials leads to much poorer fits for model C than for model A.
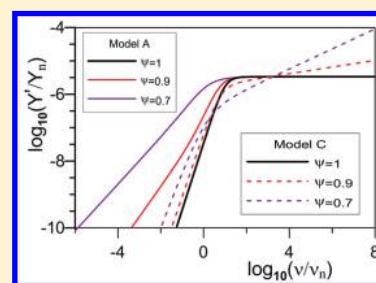
1. INTRODUCTION

A major step in the representation of diffusion of mobile charges in liquids and solids was the introduction in 1899 of the infinite-length Warburg impedance,[1] which may be expressed as $Z \equiv R(i\omega\tau)^{-1/2}$; where ω is the circular frequency of the applied voltage, τ is the relaxation time, and R is a characteristic resistance of the response. It is thus of constant-phase-element (CPE) form with a fractional exponent, ψ, of 0.5. An extensive summary of one-dimensional fractional-power-law CPE behavior for $0 < \psi \leq 1$ appears in ref 2 and mentions pertinent work by Hopkinson and Wilson dating from 1897.

An anomalous-response generalization of the finite-length Warburg model (GFW) with the Warburg exponent of 0.5 replaced by $0 < \psi \leq 1$ (but primarily restricted to 1/2 or less) was derived in 1985[3] from a distribution of activation energies treatment, and some of its responses were explored therein. It has been available in the LEVM complex-least-squares fitting program since 1992,[4] and it may be expressed in normalized terms as $Z_{TN} \equiv Z/R = \tanh(U)/U \equiv Q_{FGW}$, where $U \equiv (i\omega\tau)^{\psi}$.

In 2001, Bisquert and Compte[5] independently generalized finite-length Warburg response using fractional derivatives in the time domain and provided impedance expressions for comple-tely blocking and nonblocking electrodes, there termed reflecting and absorbing boundary conditions, respectively. Subsequently,

results were published for ordinary diffusion in thin layers and included a type of diffusion−recombination.[6] But neither this nor the earlier analysis included satisfaction of Poisson's equation and did not refer to earlier work that included arbitrary mobilities of charges, generation-recombination effects, satisfaction of the Poisson requirement, and general boundary conditions.[7−9]

Here we shall be primarily concerned with just Pois-son−Nernst−Planck (PNP) models that satisfy Poisson's equa-tion in material of finite length, full dissociation of mobile charges of equal mobilities, and completely blocking electrodes. A normal-diffusion treatment of this and more general situations appeared in 1953[10] and its impedance was first discussed in detail in ref 11; see also refs 7−9. Only recently, however, have finite-length fractional anomalous diffusion (PNPA) models been proposed and their responses explored.[12,13] The derivations, physical plausibility, and responses of these models, including fitting of experimental data, are described in the following sections. Responses of both the present simplified PNP/PNPA model and the full one that includes all the possibilities cited in the paragraph above are included in ref 13 and in the current version of the LEVM Impedance Spectroscopy fitting model.[4]

In section 2 we derive and compare several different equations for the total and interface impedances of ordinary and anomalous diffusion situations and discuss three possible response models expressed in terms of common normalized parameters. The detailed responses of the significant models A and C are presented and compared in section 3, while their adequacy in fitting three different experimental frequency-response data sets is compared in section 4. Section 5 presents conclusions following from the comparisons and fits.

2. COMPARISONS OF EQUATIONS

Here we are interested in fractional-type diffusional response appropriate for regions of finite length. The finite-length Warburg expression may be written $Z \equiv R \tanh(W)/W$, with $W \equiv (i\omega\tau)^{1/2}$, where $\tau = L^2/D$ and thus involves the length, L, between electrodes and the diffusion coefficient, D, of a diffusing mobile charge. An important parameter is $M \equiv L/(2L_D)$, the number of Debye lengths, L_D, in half the electrode separation, often of the order of 100 or more for typical experimental situations and materials. Next, set $S \equiv (i\omega\tau)$; $U \equiv S^\psi$; $P \equiv p^2 \equiv 1 + U$; $q \equiv Mp$; and $Q \equiv \tanh(q)/q$; with $0 < \psi \leq 1$.

As discussed and illustrated in ref 8, it is particularly appropriate to derive model expressions in terms of a normalized interface impedance part, $Z_{iN} \equiv Z_i/R$, and the nondiffusive high-frequency limiting conductance, G_∞, and cell capacitance, C_∞, parameters, with $R = R_\infty \equiv 1/G_\infty$. Here "interface" designates all of the response except that of the high-frequency bulk elements G_∞ and C_∞. It thus involves diffusion in the interface regions near electrodes for large M but involves the entire region between electrodes for $M < 1$. The corresponding equivalent circuit for complete blocking consists of C_∞ in parallel with the series combination of Z_i and R_∞.[8,11] In this case, the τ present in $S \equiv (i\omega\tau)$ is just $R_\infty C_\infty \equiv R_\infty (A/L)\varepsilon_V\varepsilon_\infty$, where A is the area of a plane-parallel electrode, ε_∞ is the high-frequency-limiting dielectric constant, and ε_V is the permittivity of vacuum. It then follows that the full and interface normalized impedances are connected by the relations

$$Z_{TN} = 1/[S + 1/(1 + Z_{iN})] \qquad (1)$$

and its inverse

$$Z_{iN} = [(1 + S)Z_{TN} - 1]/[1 - SZ_{TN}] \qquad (2)$$

For reference, it will be useful to list the expressions for Z_{TN} and Z_{iN} for the normal $\psi = 1$ PNP situation,[11,13] model N, before considering anomalous diffusion ones. Then $U \rightarrow S$, $P_1 \equiv 1 + S$, and the appropriate Q function will be denoted Q_1. From eq 1 in ref 11 transformed to involve the present simplified notation, and the use of eq 2, one obtains

Model N.

$$Z_{TN} = (S + Q_1)/(SP_1) \qquad (3)$$

and

$$Z_{iN} = P_1 Q_1/[S(1 - Q_1)] \qquad (4)$$

Surprisingly, for diffusion in thin films with a type of recombination but without satisfaction of the Poisson equation, Bisquert obtained for nonblocking electrodes an expression for Z_{TN} in just the form of Q_1, with somewhat different parametrization (ref 6, eq 53). Equation 4 reduces to Q_1 only for $|S| \gg 1$ and $|Q_1| \ll 1$.

Although many instances of the possible presence of anomalous diffusion, often involving fractional diffusion equations,

have been recognized and some are summarized in refs 5 and 14−17 only in refs 12 and 13 have analyses been carried out for finite-length PNP situations with Poisson-equation satisfaction. That of ref 12 led to model C and involved solution of the differential equations of the problem with the replacement of the usual time derivatives by fractional ones.[18] Although fractional diffusion equations have been used to describe anomalous diffusion situations,[14−17] until the recent derivation of model C[12] they have not been used to generalize the PNP model of ordinary diffusion where satisfaction of the Poisson equation is required. Alternatively, the work of ref 13 generalizes eq 4, the differential equations solution for the interface part of the normal PNP diffusion response, by changing all frequency response parameters in it from S to U, resulting in eq A.11 of ref 13 and eq 5 below, an expression for Z_{iN}, and a part of

Model A.

$$Z_{iN} = PQ/[U(1 - Q)] \qquad (5)$$

and

$$Z_{TN} = (U + Q)/[UP_1 + (S - U)Q] \qquad (6)$$

results that yield those of model **N** for normal diffusion. The plausible but empirical rationale for the transformation of eq 4 to eq 5 is that an interface response function for anomalous diffusion should involve only fractional frequency response parameters.

Unfortunately ref 13 unwittingly included an incorrect version of eq 6 in its eqs A.12 and A.13. It is here designated model B and is mentioned for correction and also to allow its responses to be readily compared with those of models A and C. Fortunately, all model A numerical results in ref 13 used eqs 5 and 1 rather than eq 8 below and so do not suffer from its incorrectness. Alternatively, the direct use of eq 6 yields the same numerical results for model A.

Model B.

$$Z_{iN} = P_1 Q/[S(1 - Q)] \qquad (7)$$

and

$$Z_{TN} = (S + Q)/(SP) \qquad (8)$$

Finally, eq 10 in ref 12 with the present parametrization leads through eq 2 to

Model C.

$$Z_{iN} = [P_1 Q + (U - S)]/[S(1 - Q)] \qquad (9)$$

and

$$Z_{TN} = (U + Q)/(SP) \qquad (10)$$

Although eq 10 here is parametrized differently than is eq (10) of,[12] they both represent Model C equivalently, as further discussed in the following section. Further, in the PNP limit, all the responses of Models A, B, and C properly reduce to those of Model N.

3. COMPARISONS OF RESPONSES

Responses of the A and C model equations are of particular interest for the impedance (Z), admittance (Y), and dielectric (ε) immittance levels. As discussed in the Appendix, section A.1 of ref 13 a constant nonzero low-frequency-limiting value of the real part of the impedance, Z', can appear even for completely blocking conditions and is sometimes erroneously identified as
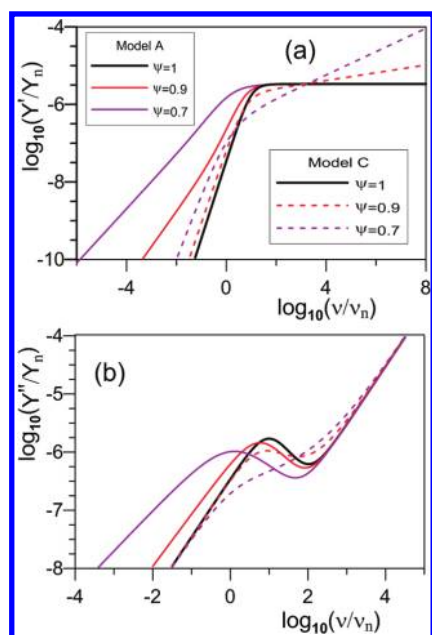
7649

dx.doi.org/10.1021/jp200737z |J. Phys. Chem. C 2011, 115, 7648–7655

Figure 1. log−log $Y'(\nu)$ and $Y''(\nu)$ PNPA responses for $\psi = 1$, 0.9, and 0.7 values. Here for the A model the $\psi = 0.7$ $Y'(\nu)$ and $Y''(\nu)$ lines deviate most from the $\psi = 1$ ones at the low-frequency extreme, while for the C one these lines deviate most at high frequencies. Here $Y_n = 1$ S, and here and elsewhere $\nu_n = 1$ Hz.

Figure 2. log−log $Z'(\nu)$ and $-Z''(\nu)$ PNPA responses for $\psi = 1$, 0.9, and 0.7 values. Note the differences in (log−log) slopes for the A and C models at high frequencies. Here $Z_n = 1$ Ω.

the DC resistance. Even then, however, no nonzero value of the real part of the conductance, $Y' \equiv G$, appears at the lowest frequencies measured, but it does so when the limiting conductance is nonzero, indicating partial blocking conditions and leading to the proper DC resistance of $1/G$ when G is nonzero.

We shall first explore full responses and then briefly discuss normalized interface ones. To do so, we use nearly the same parameter value choices as those in refs 13 and 19, but slightly changed as in ref 12. Thus, the original concentration of dissociable elements, N_0, is decreased to 4×10^{14} cm^{-3}, and although the other parameters values remained the same as those for the actual calculations in ref 12, the value of the assumed diffusion constant, D, listed therein, was incorrect. In CGS units, the actual parameter values selected were electrode separation $L = 2.5 \times 10^{-3}$ cm; electrode area, A, 2 cm^2; diffusion coefficient $D = 8.2 \times 10^{-7}$ cm^2/s; $T = 290.1$ K; and a high-frequency-limiting value of $\varepsilon_\infty = 6.7$. From the Einstein relation and the D value, the mobility value of the positive and negative fully dissociated charges was 3.28×10^{-5} cm^2/(V s). In ref 12 the fractional exponent is designated γ, while ψ is used for this quantity in LEVM[13] and herein.

The above parameter values were used in the H-circuit of LEVM to calculate exact $Z(\nu)$ PNP values for a wide frequency range, and these numerical results were then fitted with the simple $\psi = 1$ PNP model defined by the NELEM = 9 choice in the LEVM program. An exact fit resulted in the parameter values $R_\infty = 2.973 \times 10^5$ Ω, $\tau = 1.411 \times 10^{-3}$ s, and $M = 116.2$. The resulting C_∞ value is 4.746×10^{-10} F. In Figures 1−3 we present PNP/PNPA responses for the A and C circuits with $\psi = 1$, 0.9, and 0.7, all with the above other parameter values. There is necessarily some overlap with corresponding model A PNPA results presented in ref 13.

Figure 1 shows, as expected, that all the PNP and PNPA responses involve complete blocking conditions. But especially
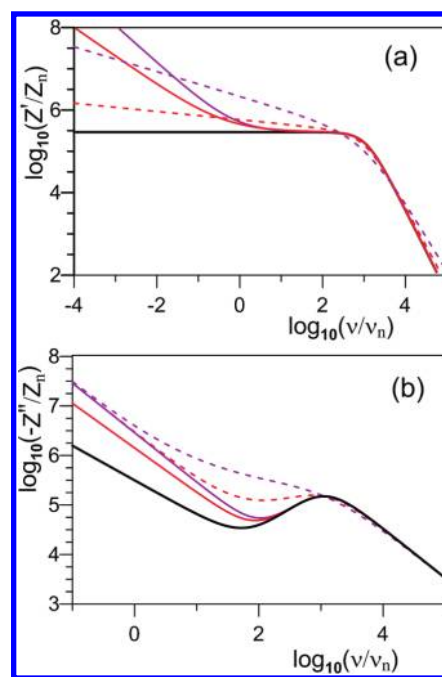
significant, however, is the model C fractional response present at frequencies above about 1 Hz. For both PNP and PNPA responses, this is here the domain of the frequency-independent R_∞ and C_∞ parameters. It therefore seems unlikely that proper PNPA response should lead to such behavior in this region, and the model A results do not do so. This unlikely behavior may be related to the extension considered for the diffusion equation which is expected to be useful for a system with anomalous spreading characterized by one fractional index, as in the situations worked out in refs 14 and 15. In fact, the fractional diffusion used to extend the standard PNP model has, in the absence of drift terms, a mean square displacement given by $\langle (x - \langle x \rangle)^2 \rangle \propto t^\psi$, where x denotes the spatial coordinate, by taking free boundary conditions into account. Situations characterized by different diffusive regimes where model A may not be appropriate may require that additional features be incorporated in this simple extension based on the fractional diffusion equations proposed in refs 14 and 15.

Comparison of the Figure 1 $Z(\nu)$ responses of ref 12 for $\psi = 1$ with the corresponding PNP response of the present Figure 2 shows that they are identical, although the Figure 1 graph is of linear−log form and $Z''(\nu)$, rather than $-Z''(\nu)$, is plotted there. Unfortunately however, the $\psi = 0.7$ C model numerical results of Figure 1 in[12] are quite different from those of the present Figure 2, and it has been established that the former employed some incorrect parameter choices for that model. Therefore, the only appropriate numerical finite-length PNPA results available so far are those in ref 13 for the A model and the present ones for A and C models.

The Figure 3 results shown here for PNPA dielectric-level response again show somewhat unlikely fractional behavior for the C model above 100 Hz but do, however, eventually lead to the proper ε_∞ high-frequency-limiting value at sufficiently high frequencies. It is interesting that ref 13 involves an incorrect
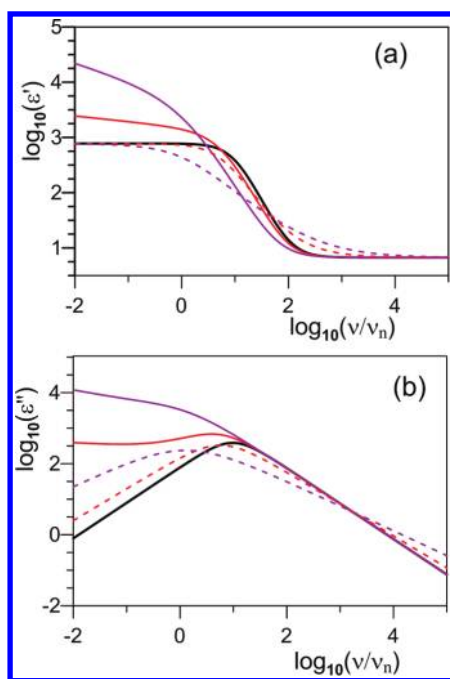
Figure 3. log−log $\varepsilon'(\nu)$ and $\varepsilon''(\nu)$ PNPA responses for $\psi = 1$, 0.9, and 0.7 values.
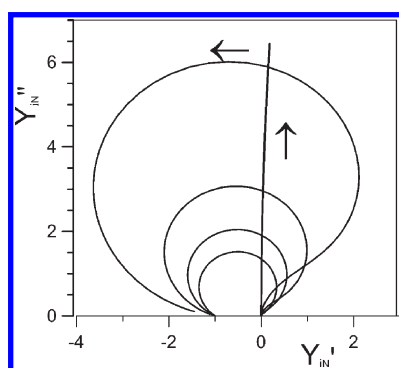

Figure 4. Y_{iN}' and Y_{iN}'' model C complex-plane interface responses for $\psi = 1$, 0.9, 0.8, 0.7, and 0.6 values. Arrows show the direction of increasing frequency.

Z_{TN} equation but proper numerical results while ref 12 involves its appropriate Z_{TN} equation but inappropriate numerical results for $\psi < 1$. It has been found, however, that the scaling factor used in ref 12 for generating the $\psi = 0.7$ numerical response shown in its Figure 1 can be amended to produce results equivalent to those shown here.

Figure 4 depicts the interface normalized Y_{iN} complex-plane responses of the C model for $\psi = 1$, 0.9, 0.8, 0.7, and 0.6. The arrows show the directions of increasing frequency. The vertical line includes the beginning of the PNP $\psi = 1$ response which properly approaches the x axis with a slope of 90° in the low-frequency limit. The large PNPA $\psi = 0.9$ curve shows at the right a start of an approach toward the $\psi = 1$ line, but it is not until ψ is of the order of 0.9999 or larger that the line begins to well approximate the $\psi = 1$ line.

Note especially the surprising negative values of Y_{iN}' apparent in Figure 4. They are a consequence of the incomplete separation of interface fractional diffusion effects and high-frequency-limiting

effects in eq 9 and raise doubt about the appropriateness of this equation, since when negative resistances appear in real situations they lead to unstable response. Again, this behavior may possibly be related to considering only a single anomalous regime in the derivation of model C, which reinforces the need to incorporate additional changes to the model C, and, as stressed before, to try to avoid such unlikely behaviors. In contrast, it is noteworthy that the model A Y_{iN}' and Y_{iN}'' both show power-law frequency behavior with low-frequency exponents (slopes) of ψ up to a frequency of about 1000 Hz followed by higher frequency ones of $\psi/2$.

The model C results, including the negative values of $Y_{iN}'(\nu)$ present in Figure 4, seem physically implausible, and it thus seems possible that the empirical replacement of ordinary time derivatives by fractional ones in the equations of motion used in deriving the C model eq 10 in ref 12 is inappropriate. It might be interesting to see if the alternate replacement of the spacial derivatives by fractional ones might lead to more reasonable results, where the exponent value might be related to the substrate of the material and possibly to the mechanism of continuous-time, random-walk (CTRW) behavior. Another possibility is that the normal Fick's law is written by assuming small spatial variation of the mobile-charge concentration. But close to a limiting surface in the presence of an external field, the bulk density of ions changes appreciably over a mesoscopic length region. In this situation, the standard Fick's law may be questionable. A possible generalization could be incorporated by expanding the current density up to cubic terms in the first spatial derivatives or in the second-order derivative.

4. EXPERIMENTAL DATA FITS

4.1. Background. Despite the apparent implausibility of the model C results, it is worthwhile to compare how well the A and C models can fit appropriate experimental data, since the presence of the same free parameters in both types of fit may be expected to lead to maximum agreement. To do so, we use the LEVM complex nonlinear least-squares (CNLS) fitting program to fit frequency-response data for three disparate materials: a hydrogel, a polymer, and one exhibiting "colossal" dielectric constant behavior. Since the responses of all these materials seem to involve partial rather than complete blocking, one needs to extend PNP and PNPA models to accommodate such behavior. The most appropriate fitting models were found to be the GPNPA, the PNPA·Deb, and the PNPA·R_S, ones used with the A and C versions of the PNPA. The free parameter G denotes a conductance ($G \equiv 1/R_P$) or conductivity ($\sigma_P \equiv 1/\rho_P$) in parallel with the full PNPA model;[13] Deb is an impedance-level Debye model (a resistance and capacitance in parallel) in series with PNPA; and R_S here represents a frequency-independent resistivity, ρ_S, in series with the PNPA. The version of the PNPA model used here does not include the presence of an adsorbed intermediate species at the electrodes or of the Chang−Jaffe electrode boundary conditions.[8,13,20]

Two different interpretations of these extensions need some discussion and will be illustrated for the GPNP response function for fully dissociated charge carriers of equal mobility. Either the addition of G introduces a new conduction path entirely separate from those of the PNPA or G involves the same mobile charge carriers and thus the same activation energies as those of the PNPA. Extrapolation to high and low frequencies using appropriate GPNPA fit parameters showed for the first case that the

$\rho'(0)$ plateau value was just $\rho_P \equiv 1/\sigma_P$; the midfrequency ρ' plateau value was ρ_∞; the DC conductivity, $\sigma'(0)$, was σ_P; and the high-frequency conductivity plateau value, σ_∞, was $(\sigma_P + \rho_\infty^{-1})$, all independent of ψ. Also as expected, the conductivities are in parallel and the equivalent resistivities are not in series. There is no DC conductivity for the present completely blocking PNPA model alone, and for small blocking (high reaction rate at the electrodes), ρ_P becomes small and eventually dominates the $\rho'(\nu)$ response over the full measured range.

The situation is different and more usual when G is used to exactly or approximately represent variable blocking of PNP charge carriers. In previous work (e.g., refs 8, 11, and 20), electrode reaction-rate parameters, (ρ_p,ρ_n), were introduced for positive and negative charges. They are based on the Chang—Jaffe boundary conditions[20] and are consistent with the Butler—Volmer equation for unbiased, small-signal conditions. For the present situation, they are real quantities[8,13] and for (0,0) lead to complete blocking, and for (∞,∞) to no blocking. In the latter case, $Z_i = 0$ and the impedance involves a maximum two-mobile resistance, R_∞ (resistivity ρ_∞), in parallel with the geometrical capacitance, $C_g \equiv C_\infty$.

A common situation is the $(0,\infty)$ one, where the negative carriers are not blocked. As shown in Figure 1b of ref 11, an exact equivalent circuit for this situation involves the parallel combination of the geometrical capacitance and $2R_\infty$ (that for negative charges only), and that combination in parallel with the series connection of $2R_\infty$ and Z_i, the interface impedance for completely blocked positive charges. The present GPNP model leads to just such a response with typical input parameter choices of $R_\infty = R_P = 2 \times 10^4\ \Omega$. The midfrequency plateau value is then just the proper R_∞ value of $10^4\ \Omega$, the parallel combination of the two resistivities, and the low-frequency plateau value is $2 \times 10^4\ \Omega$, that of R_P alone.

When the input R_P parameter value is much greater than the input R_∞ value, a partial blocking situation with ρ_n finite, the plateau values are then just R_P and R_∞, as expected from conservation of charge considerations. Further, as R_P continues to increase, the time constant defining the low-frequency end of the midfrequency plateau and the beginning of the low-frequency one, given by MC_gR_P, soon falls below the lowest measurement frequency and approaches zero in the limit of large R_P.

In refs 8 and 21 detailed expressions are listed for the full response for PNP situations under (ρ_p,ρ_n) and $(0,\rho_n)$ conditions. They simplify greatly for fully dissociated one-mobile and two-mobile situations with equal or unequal mobilities.[13] In the one-mobile case, eqs 24 and 40 of ref 8 show that the GPNP model without (ρ_p,ρ_n) terms is fully consistent with the full PNP solution for any M value, and leads to $R_P = R_\infty(1 + \rho_2^{-1})$, where $\rho_2 \equiv \rho_n$. Further, for arbitrary two-mobile conditions the more general relation, $R_P/R_\infty = R_{DN}$, follows from eq 25 of ref 8.

All fits were carried out with the data in specific form. It is convenient to define and use statistical measures of goodness of fit. We thus combine the relative standard deviation of the residuals of the fit, S_F, with the root mean square average of the relative standard deviations of the free parameters, denoted PDRMS in LEVM, to form the quantity S/P. Its values will be expressed in percent. Thus if $S_F = 0.05$ and PDRMS = 0.03, S/P would involve 5 and 3. In these fits we use proportional weighting[4,13] so that fits at the impedance and complex modulus level then yield the same value of S_F, while those at the

admittance and dielectric-constant levels are the same but generally different from the other one except in the limit of fitting a model to exact data derived from it. When the difference is significant, it is another measure of the inappropriateness of a model for the data fitted, and we shall therefore list the values of $(S/P)_\sigma$ and $(S/P)_\rho$ for each A and C fit. Both parts of S/P are important and are 1 or less for excellent fits, and 10 or more for poor ones. Note that a single poorly defined parameter will dominate the PDRMS value even when other well-defined parameter estimates are present.

4.2. Hydrogel Fits. We begin with an analysis of the frequency response data for a gel composed of 1% ethylene glycol, 1% hydroxyethylcellulose, and 98% depurated water, previously considered in ref 13. The data considered there still contained some obvious outlying points, most of them now removed in order to obtain somewhat improved fits. The model A GPNPA results shown in row 1 of the present Table 1 are still comparable, however, to those in row 6 of Table 1 of ref 13, and both involve the data in specific form. Of the several model A fits carried out at the ρ level, the GPNPA one of row 1 was somewhat superior to other choices. For example, the S/P values for PNP, PNPA, GPNP, and PNPA·Deb choices were 17/3.5, 6.9/4.0, 9.3/3.3, and 4.0/7.7, respectively.

Comparison of the models A and C GPNPA fit results are presented in rows 1 and 2 of Table 1 and in Figure 5. In these log—log plots there is little or no deviation evident between the data lines and those of the model A fit, but one notices particular discrepancies between the data and the model C fit lines, particularly at low frequencies. This is reflected in the S_F goodness-of-fit values shown in the table where those for C are more than twice as large as the A ones. Especially noteworthy is the model C estimate of ψ of nearly unity (very close to PNP response). It appears that the CNLS C fit requires such a value of ψ to ensure good fitting of the high-frequency responses, but this results in worse fitting of the low-frequency ones, a failing not present for the A model fits.

It was shown in ref 13 using the LEVM H-circuit fitting approach that the measured electrode separation, L, when taken as a free parameter only led to its proper known value when the fit model involved the two-mobile case of fully dissociated positive and negative charges of equal mobilities. A fit of the present purged data with the H circuit yielded the same conclusion as well as exactly the same A model fit and parameter estimates shown in row 1 of Table 1. The values of the charge concentration, N_0, and mobility, μ, however were different and are $1.07 \times 10^{17}\ cm^{-3}$ and $3.19 \times 10^{-3}\ cm^2/(V\ s)$, respectively, indicating less free charge and greater mobility than in the earlier estimates.

4.3. Polymer Electrolyte Fits. Frequency response data sets for a polymer electrolyte containing polyethylene imine (PEI) and lithium bis(trifluoromethylsulfyl imide (LiTFSI) were kindly supplied by Professor G. A. Niklasson.[22] They have been discussed by him and his group in ref 23. Here we consider the data set with a [N]:[Li] molar ratio of 400:1 at 20 °C and fit it with different models than those utilized in ref 23. The electrode separation was 3.1 mm. Note that the $\sigma'(\nu)$ response increases at high frequencies as shown in Figure 6a, unlike that of model A, but similar to that of model C in Figure 1a. There is no such rise for the gel data of Figure 5a, so the present data set provides a useful opportunity to evaluate how well model C can fit data with such a high-frequency increase.

Fit comparison results are shown in rows 3—5 in the table and in Figure 6. We see that although the A model fit is quite good,

7652

dx.doi.org/10.1021/jp200737z |*J. Phys. Chem. C* 2011, 115, 7648—7655

Table 1. Results of Proportional Weighting CNLS Fits of Complex $\sigma(\nu)$ and $\rho(\nu)$ Specific Data Sets for a Hydrogel, a Polymer, and $CaCu_3Ti_4O_{12}$ (CCTO), Using the A and C Models Defined in Section 2 with GPNPA (rows 1, 2, 6, 7), PNPA·Deb (rows 3, 4), and PNPA·R$_S$ (row 5) Fitting Functions[a]

no.	material and model	(S/P)	$(S/P)_\rho$	ρ_∞ ($\Omega\cdot$cm)	τ_0 (s)	M	ψ	ρ_P or $[\rho_S]$ ($\Omega\cdot$cm)	ρ_D ($\Omega\cdot$cm)	τ_D (s)	ε_∞ from fits
1	HydroGel	4.1	4.2	9.2×10^3	9.0×10^{-8}	9.7×10^3	0.885	6.2×10^4			110.9
	A	3.8	3.5								
2	C	8.6	8.8	9.9×10^3	9.7×10^{-8}	2.5×10^4	0.998	4.0×10^4			110.4
		3.7	2.9								
3	polymer A	1.9	1.7	1.9×10^5	2.7×10^{-7}	8.4×10^4	0.896		7.6×10^5	1.2×10^{-6}	8.45
		4.4	4.3								
4	C	5.4	4.8	1.5×10^5	2.4×10^{-7}	2.6×10^5	0.997		7.9×10^5	1.1×10^{-6}	8.27
		13	13								
5	C	6.5	5.6	9.0×10^5	9.7×10^{-7}	3.8×10^5	0.999	$[5.7\times10^4]$			12.2
		6.1	4.6								
6	CCTO A	2.0	2.4	1.3×10^3	1.6×10^{-8}	508	0.902	4.2×10^4			132
		1.6	1.9								
7	C	16	16	1.2×10^3	3.6×10^{-9}	5000 F	0.966	4.5×10^5			37
		3.6	5.6.								

[a] The Debye parameters are designated ρ_D and τ_D. Goodness of fit values for S/P are listed for both σ- and ρ-level fits, but model parameter estimates are shown here only for the latter. For these specific data sets the parallel conductivity, σ_P, denoted by G in the model name, is replaced in the table by its inverse ρ_P. The ε_∞ values listed in the rightmost column were calculated from the parameter estimates of the ρ-level fits. The row 7 anomalous CCTO fit using the C model necessarily involved a fixed value of M, as discussed in the text.
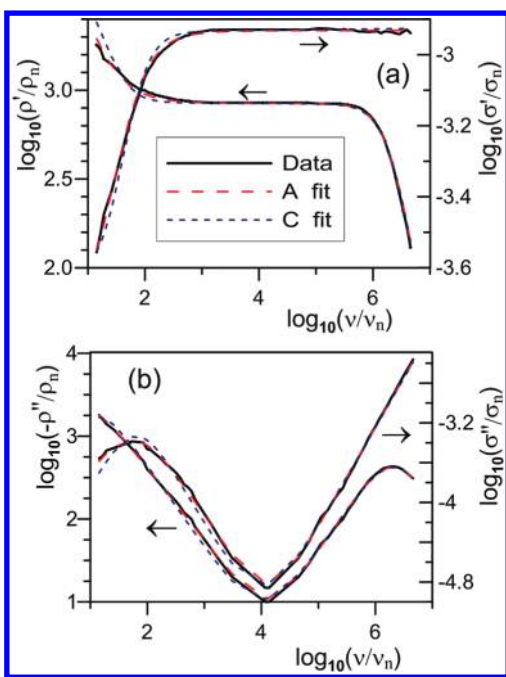

Figure 5. Comparisons of model A and C fits of room-temperature hydrogel data at ρ and σ immittance levels: (a) real parts; (b) imaginary parts.

Figure 6. Comparisons of model A and C fits of 400:1 PEI-LiTFSI 20 °C polymer data at ρ and σ immittance levels: (a) real parts; (b) imaginary parts.

the two C model ones are more dubious. The PDRMS values listed in row 4 are very large and are indicative of large uncertainties of the PNP parameters of columns 5 and 6. Further, although the PNPA·R$_S$ fit of row 5 is appreciably better, it turns out that this model leads at high frequencies to a nonphysical continual decrease in $\varepsilon'(\nu)$ beyond a plateau. The ε_∞ value listed in the last column of this row is the plateau value, appreciably different from the values in rows 3 and 4, which themselves are
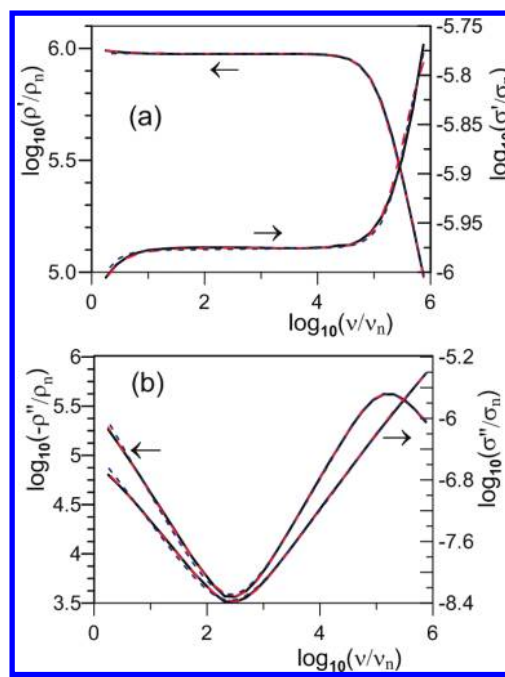
close to those independently estimated in ref 23. Therefore, the C model results shown in Figure 6 are those for the PNPA·Deb fits of rows 3 and 4. We see that although the C model led to nearly as good fits of $\sigma'(\nu)$ as did model A at high frequencies, its resulting ψ values were exceedingly close to unity; PNP response and the PNPA part of the response model thus contributed virtually nothing to the high-frequency rise in $\sigma'(\nu)$.

Further model A fits of this data set were carried out using the H-circuit in LEVM. They were found to lead to the same S_F value
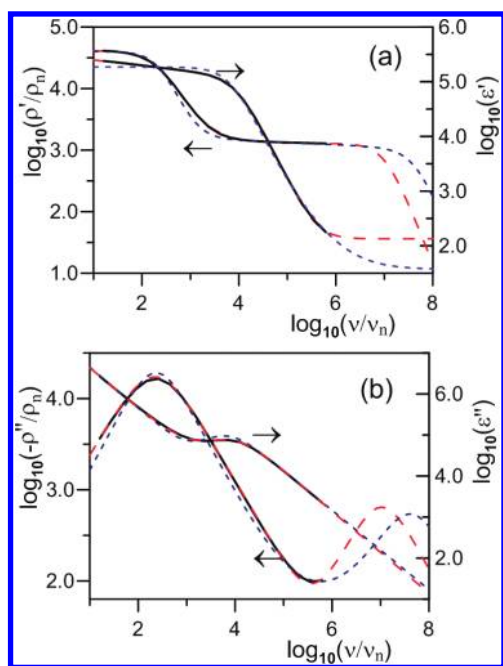
7653

dx.doi.org/10.1021/jp200737z |J. Phys. Chem. C 2011, 115, 7648–7655

Figure 7. Comparisons of model A and C fits of 140 K CaCu$_3$Ti$_4$O$_{12}$ data at ρ and ε immittance levels: (a) real parts; (b) imaginary parts. The responses above about 10^6 Hz are extrapolations using the lower-frequency fit parameters.

as that in row 3, column 4 of the table for both charge of one sign mobile and for both signs equally mobile for full dissociation conditions. All parameters common to the A model fit of row 3 were also the same. The mobility was reasonably well estimated to be about 4.87×10^{-4} cm^2/(V s) and the ε_∞ estimate for the PNPA part of the fit model was 16.6. The N_0 estimates were, however, 6.90×10^{16} and 3.45×10^{16} cm^{-3}, respectively. Further, although the M value for the two-mobile situation agreed with that in row 3, that estimated from the one-mobile fit was $2^{1/2}$ larger. It thus appears likely that the two mobile choice is the more appropriate one for this material, but it should be understood that the fit model used does not allow discrimination of more complicated conduction processes with more than two species of mobile charge.

4.4. CaCu$_3$Ti$_4$O$_{12}$ Fits. Dr. Peter Lunkenheimer kindly provided data sets for the frequency response of CaCu$_3$Ti$_4$O$_{12}$ (CCTO) in single-crystal form with sputtered gold electrodes,[24,25] and here we fit the one at 140 K. This material is a "colossal" dielectric constant one that exhibits high mobility, and so we present ρ and ε plots here rather than ρ and σ ones. Because the CCTO data sets were known to contain appreciable errors above 10^6 Hz, we limit the present one at that point, but after fitting we use the fit parameters to extrapolate the fits to 10^8 Hz.

Results are shown in rows 6 and 7 of Table 1 and in Figure 7. Unfortunately, when all the GPNPA parameters of the C model fit were taken free, no valid fit was possible; instead estimates of the parameters of columns 5−7 were completely uncertain. But when M was held fixed, an adequate fit became possible. The results were not very sensitive to the fixed value of M, but that used in column 7 of the table gave a slightly better fit than did other much smaller or bigger ones. As shown in Figure 7, even with the constrained value of the C model M parameter, its results are again much inferior to those of model A. Also,

although the model A fit of row 6 was quite good and led to an estimate of ε_∞ close to that apparent in Figure, 1 of ref 25, the extrapolated model C ε_∞ estimate was much smaller.

The results of H-circuit LEVM fits of the present data were particularly interesting and instructive since they provided separate estimates of further model A parameters. These fits clearly showed that the data were best represented by equal charge-valence numbers and very small charge dissociation. With the bulk concentration of dissociable entities, N_0 was held fixed at its fit value, equal S/P values of 2.39 and 1.39 were obtained for both one-mobile and two-mobile situations, and all parameter estimates common to the model A fit of row 6 were the same for the two-mobile situation, but as expected, the M estimate in the one-mobile case was $2^{1/2}$ times larger than that for the two-mobile estimate.

For both situations, the mobility was estimated as 62.8 cm^2/(V s), a value so large that one must conclude, as in ref 25, that the conduction in the material is electronic, not ionic. But unlike the treatment in ref 25 which suggested Schottky-diode behavior (see, e.g., ref 26), we here fit the data more precisely with the PNPA model involving diffuse double layer formation at the electrodes.

When the mobility ratio parameter, Π_m, was set free to vary with a starting value of unity, the fit led almost exactly to unity, but when its starting value was of the order of 10^5, its fit estimate was about 10^7, nearly one-mobile response, but very poorly estimated. Therefore, the one-mobile fit was carried out with a fixed value of Π_m of 10^{25} or greater. For the two-mobile case, the N_0 and the dissociation ratio, $D_D \equiv c_0/N_0$,[13] were 3.57×10^{21} cm^{-3} and 1.052×10^{-8}, respectively. For the one-mobile case, these values were exactly 4 and 0.5 times larger/smaller, respectively. Here c_0 is the common concentration of the mobile charges in the two-mobile case, and n_0 is the concentration of the mobile negative charges in the one-mobile situation. Their values were about 3.755×10^{13} cm^{-3} and 7.51×10^{13} cm^{-3}, respectively. Although the fits were unable to yield different mobilities for the positive and negative charge carriers, presumably holes and electrons here, they do suggest that the two-mobile situation is indeed more appropriate for this material than is the one-mobile one.

5. CONCLUSIONS

Two distinct, physically plausible empirical generalizations of PNP ordinary diffusion in a cell with plane-parallel electrodes to anomalous PNPA diffusion have been expressed in simplified notation for comparison of their full impedance expressions as well as their interface parts. Some different methods of taking account of partial blocking of charge carriers at the electrodes have also been discussed, compared, and used herein for the fitting of relevant experimental data.

Examination of the differences between the A and C models and CNLS fitting using them for data sets for three different materials involving partial blocking of charge carriers showed that the A model was both physically more plausible and led to far better fits than did the C one, which involved the ab initio introduction of fractional time derivatives in the basic differential equations involving charge motion. In addition, we showed that the A model led to good fits of two experimental data sets with fully dissociated ionic charges of equal positive and negative mobilities, and yielded excellent fits of data for a single-crystal, high-dielectric-constant material with very small dissociation and electronic conduction.

The apparent nonphysical behavior of the C model involving fractional time derivatives arises from its failure to satisfy the basic requirement of dissipative phenomena that, on the transformation of t to $-t$, its response must change. Evidently even though the model C way of introducing fractional behavior is clearly faulty, other possibilities, including a model that combines fractional time derivatives with ordinary ones,[12] might lead to physically satisfactory results and might possibly be needed in some situations to best explain experimental data. Presently, however, model A has been shown to be both physically plausible and capable of well fitting diverse anomalous diffusion experimental results.

■ AUTHOR INFORMATION

Corresponding Author
*E-mail: macd@email.unc.edu.

■ REFERENCES

(1) Warburg, E. *Ann. Phys. Chem.* **1899**, *67*, 493. Warburg, E. *Drude Ann. Phys.* **1901**, *6*, 125.

(2) McAdams, E. T.; Jossinet, J. *Physiol. Meas.* **1995**, *16*, A1.

(3) Macdonald, J. R. *J. Appl. Phys.* **1985**, *58*, 1955.

(4) Macdonald, J. R.; Potter, L. D., Jr. *Solid State Ionics* **1987**, *23*, 61. Macdonald, J. R. *J. Comput. Phys.* **2000**, *157*, 280. The newest WINDOWS version, LEVMW, of the comprehensive LEVM fitting and inversion program may be downloaded at no cost by accessing http://jrossmacdonald.com. It includes an extensive manual and executable and full source code. More information about LEVM is provided at this internet address. All of the J. Ross Macdonald papers cited herein are available in PDF format for downloading from this address.

(5) Bisquert, J.; Compte, A. *J. Electroanal. Chem.* **2001**, *499*, 112.

(6) Bisquert, J. *J. Phys. Chem. B* **2002**, *106*, 325.

(7) Macdonald, J. R.; Franceschetti, D. R.; Meaudre, R. *J. Phys. C: Solid State Phys.* **1977**, *10*, 1459.

(8) Macdonald, J. R.; Franceschetti, D. R. *J. Chem. Phys.* **1978**, *68*, 1614. See also pp 4-9, 4-10, and 4-26 of the LEVMW manual for discussion of PNPA models available in the LEVMW fitting program.

(9) Macdonald, J. R. *J. Electrochem, Soc.* **1988**, *135*, 2274. Below eq A-1, in γ_j replace θ_j^2 by θ_j, and on p 2279 in t_1 replace ψ by $\psi^{1/2}$.

(10) Macdonald, J. R. *Phys. Rev.* **1953**, *92*, 4.

(11) Macdonald, J. R. *J. Electroanal. Chem.* **1971**, *32*, 317.

(12) Lenzi, E. K.; Evangelista, L. R.; Barbero, G. *J. Phys. Chem. Lett.* **2009**, *113*, 11371.

(13) Macdonald, J. R. *J. Phys.: Condens. Matter* **2010**, *22*, 495101.

(14) Metzler, R.; Klafter, J. *Phys. Rep.* **2000**, *339*, 1. Metzler, R.; Klafter, J. *J. Non-Cryst. Solids* **2002**, *305*, 81.

(15) Hilfer, R. *Applications of Fractional Calculus in Physics*; World Scientific: Singapore, 2000. Hilfer, R. *J. Non-Cryst. Solids* **2002**, *305*, 122.

(16) Hilfer, R.; Metzler, R.; Blumen, A.; Klafter, J. *Strange Kinetics; Chemical Physics*; Pergamon-Elsevier: Amsterdam, The Netherlands, 2004; Vol. 284, Numbers 1−2.

(17) Lenzi, E. K.; Mendes, R. S.; Tsallis, C. *Phys. Rev. E* **2003**, *67*, 0312104.

(18) Podlubny, I. *Fractional Differential Equations*; Academic Press: San Diego, 1999.

(19) Derfel, G.; Lenzi, E. K.; Yednak, C. R.; Barbero, G. *J. Chem. Phys.* **2010**, *132*, 224901.

(20) Chang, H.; Jaffe, G. *J. Chem. Phys.* **1952**, *20*, 1071.

(21) Macdonald, J. R. *J. Chem. Phys.* **1973**, *58*, 4982. Macdonald, J. R. *J. Chem. Phys.* **1974**, *60*, 343.

(22) Niklasson, G. A. Private communication.

(23) Pehlivan, I. B.; Marsal, R.; Georen, P.; Granqvist, C. G.; Niklasson, G. A. *J. Appl. Phys.* **2010**, *108*, 074162.

(24) Lunkenheimer, P. Private communication.

(25) Krohns, S.; Lunkenheimer, P.; Ebbinghaus, S. G.; Loidl, A. *Appl. Phys. Lett.* **2007**, *91*, 022910.

(26) Macdonald, J. R. *Solid-State Electron.* **1962**, *5*, 11.

7655

dx.doi.org/10.1021/jp200737z |*J. Phys. Chem. C* 2011, 115, 7648–7655